IOP PUBLISHING PHYSICA SCRIPTA

Phys. Scr. **80** (2009) 048122 (6pp) doi:10.1088/0031-8949/80/04/048122

Ultra-sensitive detection of nitric oxide isotopologues

Christoph Mitscherling, Christof Maul and Karl-Heinz Gericke

Department of Physical and Theoretical Chemistry, Technische Universität Braunschweig,
Hans-Sommer-Strasse 10, 38106 Braunschweig, Germany

E-mail: c.mitscherling@tu-bs.de

Received 15 February 2009
Accepted for publication 25 June 2009
Published 1 October 2009
Online at stacks.iop.org/PhysScr/80/048122

Abstract

This paper reviews recent technical advances of resonance enhanced multiphoton ionization (REMPI) spectroscopy and laser-induced fluorescence (LIF) spectroscopy, both extremely sensitive techniques for the determination of low nitric oxide (NO) concentrations. Because NO is involved in a multitude of biological functions, labeling and isotope-specific detection are important tools for elucidating chemical pathways. Mass selective REMPI discovers spectroscopic windows for monitoring the most abundant isotopologues such as $^{14}N^{16}O$, $^{15}N^{16}O$ and $^{14}N^{18}O$ without these species interfering spectroscopically with each other. This has been realized by using the $A^2\Sigma^+(v' = 0) \leftarrow X^2\Pi_\Omega(v'' = 0)$ transition (NO γ-band) in the ultraviolet region around 226 nm. Selected rovibrational transitions are employed for the ultra-sensitive and isotope-specific detection of exhaled NO by LIF. The detection limit for $^{14}N^{18}O$ has been improved to 0.8 parts per trillion.

Furthermore, preliminary results from a study of the $A^2\Sigma^+(v' = 1) \leftarrow X^2\Pi_\Omega(v'' = 0)$ transition interfering with the $B^2\Pi(v' = 1) \leftarrow X^2\Pi_\Omega(v'' = 0)$ transition are presented as an alternative approach for isotopologue selective measurements of $^{14}N^{18}O$. From experimental data the rotational constant $B = 1.10310\,\text{cm}^{-1}$ and the spin–orbit coupling constant $A = 33.170\,\text{cm}^{-1}$ of $^{14}N^{16}O$ ($B^2\Pi(v' = 1)$) have been calculated.

PACS number: 33.20.Lg

1. Introduction

The Nobel Prize for medicine and physiology in 1998 was awarded to Furchgott [1], Ignarro and Murad, who identified nitric oxide (NO) as a key player in mammalian blood pressure regulation [2]. As is known today, NO is involved in a multitude of physiological processes such as immune defense and brain memory [3]. The average lifetime of NO is very low under physiological conditions. Due to the role of NO in the immunological defense of the human body, the molecule is an important marker for monitoring inflammatory diseases [4] of the airways, e.g. asthma [5]. Common clinical devices achieve detection limits of about 1 part per billion (ppb), which is sufficient for exhaled NO concentrations in the range of 10–100 ppb. The main disadvantages of such devices are the relatively low temporal resolution of a few seconds and the incapability of differentiation between several NO isotopologues, which are both important aspects in medical studies concerning the metabolism behavior and reactive pathways of NO inside the body. Both aspects are significantly improved by the application of laser-induced fluorescence (LIF) [6, 7] spectroscopy as shown later on. Besides airway-originated NO a small amount is emitted by the skin, which has also been studied extensively [8]. During the last years it has turned out that NO is also involved in plant signaling [9], e.g. as a transmitter during biological and abiological stress.

The global impact of NO as part of the NO*x* cycle is of significant importance. NO is involved in ozone depletion in the stratosphere as well as ozone formation in the lower atmosphere of urban regions. Main sources of NO production [10] are fossil fuel combustion, combustion of biomass and emission from soils and plants. The overall output of NO is estimated to be around 40 MT a^{-1}. All mentioned fields of research imply extremely low local NO concentrations. Therefore, a need for very sensitive and isotopologue selective detection methods rises. The most abundant isotopic compounds of NO are $^{14}N^{16}O$, $^{15}N^{16}O$ and

$^{14}N^{18}O$ with fractions due to the natural isotopic distribution of 99.394, 0.363 and 0.204%, respectively [11].

Many methods have been recently employed for the detection of NO. In chemiluminescence measurements NO is converted to excited NO_2, e.g. by ozone [12, 13]. The quantity of fluorescence from NO_2 can be detected and related to a NO calibration procedure. This technique is mostly used in commercially distributed devices and is selective for NO with detection limits about 10 ppt to 1 ppb according to the average time. The method is not isotopologue specific. Cavity ring down spectroscopy (CRDS) is a classical absorption technique that refers to the Lambert–Beers law [14, 15]. This fast method is essentially free of calibration procedures and can be used for many different molecules. CRDS for the detection of NO is mostly done by application of infrared light which can be a problem concerning interference with other trace gases, e.g. water in exhaled air analysis. The detection limit is around 10 ppt. In laser magnetic resonance (LMR) experiments a magnetic field is applied to the sample [16, 17]. Different isotopologues can be detected with a detection limit in the ppb region. Furthermore, photoacoustic spectroscopy [18], electron paramagnetic resonance (EPR) [19] and different mass spectroscopic methods [20, 21] can be used for NO detection. We applied a combination of resonance enhanced multi photon ionization (REMPI) spectroscopy with a time-of-flight (TOF) mass spectrometer (MS) and LIF spectroscopy for the selective detection of different NO isotopologues down to concentrations in the sub-ppt region with a maximum time resolution of 20 ms.

Numerous studies have been carried out on the spectroscopy of NO, especially of the γ-band system [22–26]. Nevertheless, spectroscopic constants for the excited $A^2\Sigma^+(v'=0)$ state of the $^{14}N^{18}O$ isotopologue can hardly be found in the literature. The selective detection of NO via the $A^2\Sigma^+(v'=1)$ state is very important and will be discussed later. This state is interfered by the $B^2\Pi(v'=1)$ state, which is not well studied due to its interference with $AX(v'=1)$ [27–29]. Application of LIF spectroscopy and REMPI can help for a better understanding of these transitions. Comparison and fitting of calculated spectra to the measured ones can provide exact calculations of spectroscopic constants. Hence, these techniques can enrich both the highly sensitive isotopologue selective detection of NO in various biological environments as well as classical spectroscopic studies.

2. Detection procedure

The REMPI setup consists of a XeCl Excimer (Lambda Physik LPX 600) pumped dye laser (Lambda Physik FL 2002, operated with Coumarin 47) with a β-barium-borate crystal for second harmonic generation. Separation of the second harmonic is achieved by a setup of four Pellin-Broca prisms which finally generates 600 μJ pulses around 226.6 nm at 10 Hz. A schematic overview is given in figure 1. For the (1+1) REMPI measurement we excite the $A^2\Sigma^+(v'=0) \longleftarrow X^2\Pi_{\frac{1}{2}}(v''=0)$ around 226.6 nm as a resonant intermediate and then add another 226.6 nm photon for ionization of NO. Due to a frequency change of the dye laser NO isotopologues can be ionized selectively. The ionization takes place in a homebuilt stainless-steel cube with an integrated single-field TOF spectrometer. The TOF device has a total length of 0.57 m with a ratio of the acceleration region to the drift region of 1 : 2. The ionized NO^+ is accelerated in an electric field and detected with a multi-channel plate (MCP) in chevron arrangement. The combination of a 40 $m^3\,h^{-1}$ oil diffusion pump and a 150 $L\,s^{-1}$ turbo molecular pump evacuates the spectrometer to a base pressure of 10^{-6} mbar. A detailed description of the setup is given elsewhere [30].

Due to different flight-times of the three main isotopologues of NO ($^{14}N^{16}O$, $^{15}N^{16}O$ and $^{14}N^{18}O$ with the masses 30, 31 and 32 u) a differentiation in the MCP signal is possible. The MCP signal is gated and processed with three boxcars, each on a single NO isotopologue. The output signals are recorded by a LabView^{TM} program. This setup has been applied to reveal spectroscopic windows for the detection of single NO isotopologues. As soon as these windows could be found, an LIF device has been used for a further observation because of its higher flexibility for the application of dynamic samples as well as a higher sensitivity for NO detection.

For the isotopologue selective detection of NO, we apply the well-known γ-band system. NO is excited by $A^2\Sigma^+(v'=0) \leftarrow X^2\Pi_\Omega(v''=0)$ around 226.6 nm in the ultraviolet (UV), and subsequent detection of fluorescence from $A^2\Sigma^+(v'=0) \rightarrow X^2\Pi_\Omega(v''\geqslant 2)$ is recorded. Alternatively, the $A^2\Sigma^+(v'=1) \leftarrow X^2\Pi_\Omega(v''=0)$ transition around 215.0 nm interfering with the $B^2\Pi(v'=1) \leftarrow X^2\Pi_\Omega(v''=0)$ transition is investigated for isotopologue selective detection of NO. Due to the higher vibrational state of $^2\Sigma^+(v'=1)$, the band origins of the different NO isotopologues are more shifted against each other and therefore more suitable for selective observations.

The applied laser system for LIF experiments is identical to the previously described one for REMPI measurements. A schematic overview is given in figure 1. The output beam is directed through CaF windows in Brewster angle arrangement to the measuring cell and furthermore through a comparable reference cell. Both cells benefit from a Woods horn on the entrance and exit side as well as from two pinholes for better adjustment and reduction of scattered light. Fluorescence is collected from the excitation region by a $1/f$ lens system perpendicular to the excitation beam. Furthermore, an Ag-covered spherical mirror with focus inside the fluorescence region reflects fluorescence to the lens system. The parallelized fluorescence is spectrally filtered by a bandpass filter (Andover Corporation 248FS10-50, transmission of 0.166 at central wavelength 250.964 nm, full-width at half-maximum (FWHM) is 10.97 nm) to essentially collect fluorescence from $A^2\Sigma^+(v'=0) \rightarrow X^2\Pi_\Omega(v''=1-3)$ and amplified by a solar blind side-on photomultiplier (PM) (Hamamatsu R7154). Alternatively, a longpass filter (Glen Spectra, 238AELP) with a cut-on wavelength of 237.5 nm and a maximum transmission of about 0.9 has been applied. The PM signal with an input resistance of 50 Ω is gated by a standard boxcar arrangement (SR 250) controlled by a LabView^{TM} (National Instruments Corporation) program. The boxcar as well as the excimer laser is triggered by a delay generator (Quantum Composers 9514).

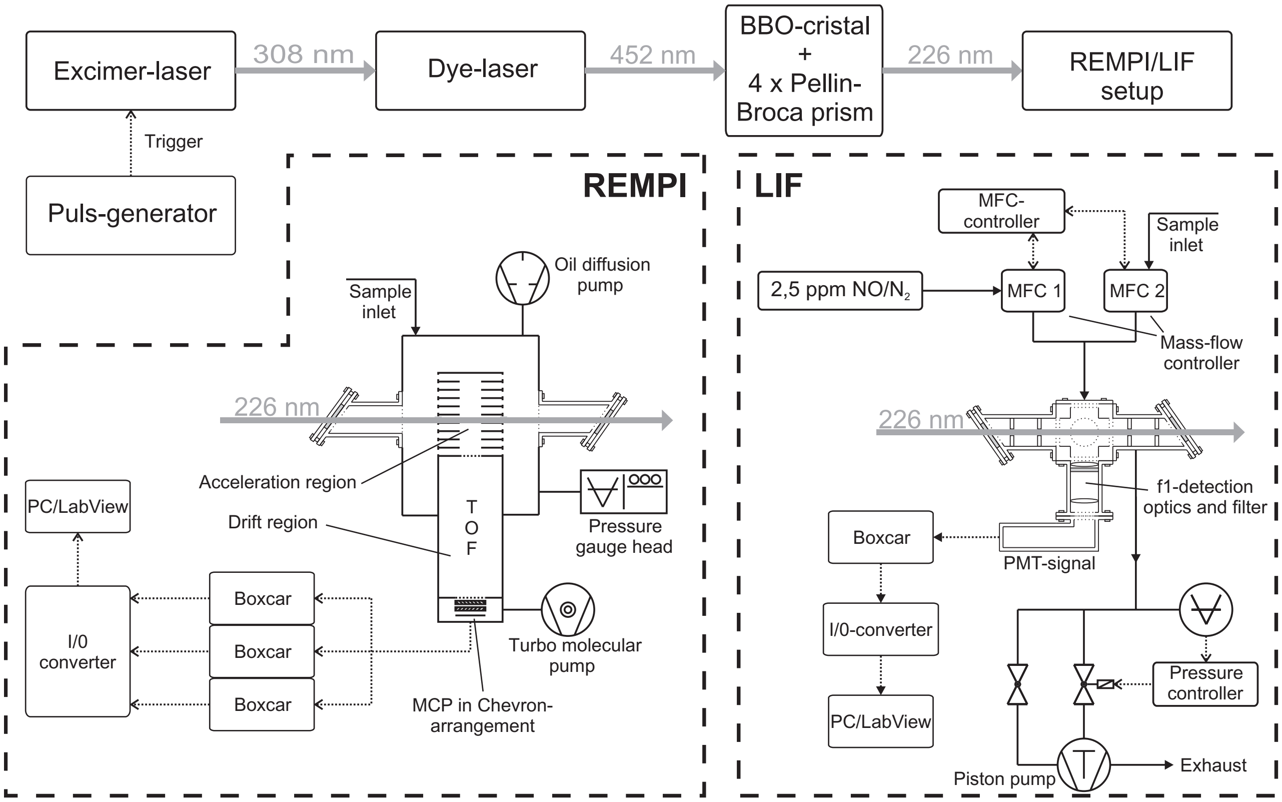

Figure 1. Schematic experimental setup of LIF and REMPI measurements. (BBO = β-barium borate crystal, TOF = time-of-flight mass spectrometer, PMT = photomultiplier tube, MFC = mass flow controller, full lines = mass flow, dotted lines = data flow.)

The mass flux system of the measuring cell is optimized for the application of variable gas flows and application of the standard addition method (SAM) for calculation of unknown NO concentrations. The mass flux controller 1 (MFC1) (MKS Instruments 1179A) can be operated with a 2.5 ppm mixture of NO and nitrogen between 0.1 and 10 standard cubic centimeters per minute (sccm min^{-1}). MFC 2 ranges from 50 to 5000 sccm min^{-1} for variable samples such as breath measurements. The vacuum system consists of a piston pump (Pfeiffer Vakuum XtraDry) in combination with a digitally controlled (MKS Instruments 250E) automatic valve (MKS Instruments 248A). For higher mass fluxes a bypass has been installed. The optimum cell pressure for fluorescence measurements is around 10 mbar. A more detailed description of the experimental setup can be found elsewhere [31].

For the determination of absolute NO concentrations two methods are applied. In principal, the amount of detectable fluorescence is proportional to the NO concentration of the unknown sample. The fluorescence signal can be evaluated by the more or less conventional application of calibration curves or the standard addition method (SAM). The main problem with calibration curves is the effect of quenching due to ambient air and trace gases [31]. This disadvantage is avoided by the SAM but large amounts of the unknown sample are required. During the SAM the signal from the unknown sample is observed continuously while different NO concentrations of a known sample are added. From this procedure it is possible to calculate very accurately the NO concentration of the unknown sample.

3. Results and discussion

The mass selective REMPI measurements have been performed to find spectroscopic windows for the interference-free detection of the most abundant NO isotopologues. We were mainly interested in $^{14}N^{18}O$ because no spectroscopic constants could be found in the literature for the excited A-state. Accordingly, an accurate calculation of line positions for this isotopologue is not possible. The MCP signal has been gated with three boxcars each on a single mass of the main isotopologues $^{14}N^{16}O$, $^{15}N^{16}O$ and $^{14}N^{18}O$ with 30, 31 and 32 u, respectively. Due to extremely strong signals from $^{14}N^{16}O$ (because of its high concentration in comparison to the minor isotopologues), the signal also appears on the mass-31-boxcar and the mass-32-boxcar signal. $^{15}N^{16}O$ and $^{14}N^{18}O$ can only be observed without strong $^{14}N^{16}O$ transitions. For the $A^2\Sigma^+(v' = 0) \leftarrow X^2\Pi_\Omega(v'' = 0)$ transition the region from 224 to 229 nm has been recorded by wavelength variation of the dye laser. A section of these measurements is displayed in figure 2. It could be shown that in certain areas of the spectra $^{15}N^{16}O$ as well as $^{14}N^{18}O$ can be observed without interference with the main compound $^{14}N^{16}O$ [30]. Simulations for all three isotopologues have been performed with the program pgopher [32]. The results of fitting procedures are in excellent agreement with measured spectra.

By application of the LIF method selected interference-free sections of the REMPI spectra have been observed in more detail. The spectral resolution of the dye laser output has been determined by a Fabry–Perot interferometer to be 7 GHz. Cross sensitivities during the

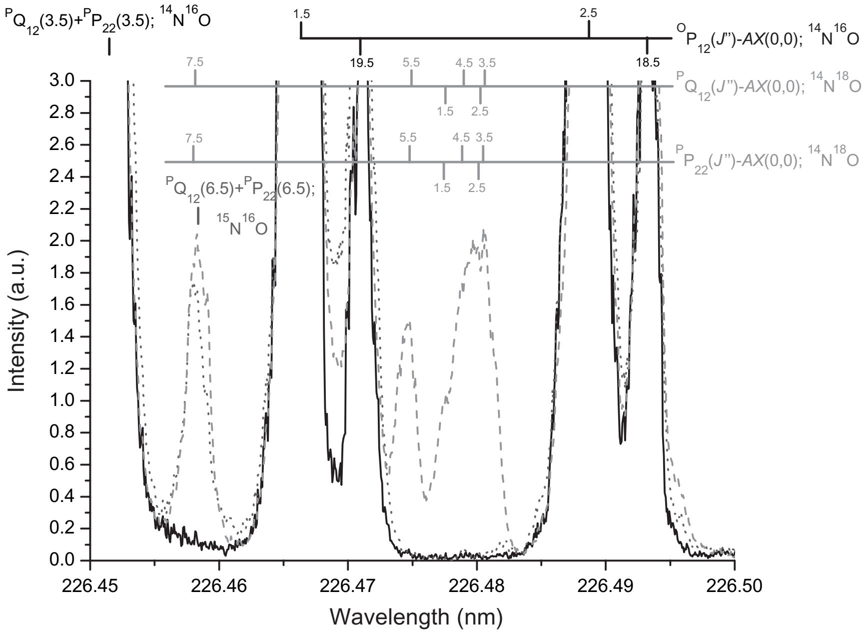

Figure 2. REMPI spectrum between 226.45 and 226.50 nm from $A^2\Sigma^+(v'=0) \leftarrow X^2\Pi_\Omega(v''=0)$ of NO (solid line = $^{14}N^{16}O$; dotted line = $^{15}N^{16}O$; dashed line = $^{14}N^{18}O$).

measurement can be excluded as discussed in [31]. A dilution series has been recorded to estimate the detection limit for NO detection. A mixture of 2.5 ppm NO in N_2 has been diluted stepwise with Ar until the detected fluorescence approached the noise level of pure Ar (value for 0 ppt). Constant excitation of the $^PQ_{12}(2.5) + ^PP_{22}(2.5) + ^PQ_{12}(3.5) + ^PP_{22}(3.5)$ transitions of $^{14}N^{18}O$ and subsequent collection of radiated fluorescence resulted in the averaged values of figure 3. The straight line is a fit of the recorded data. Each point has been averaged over 400 laser shots. The fit has been performed with a Matlab program for straight-line data with errors in both coordinates. The main causes for uncertainties of the concentration are the accuracy of the applied MFCs as well as the uncertainty of the 2.5 ppm NO mixture. Calculation of $^{14}N^{18}O$ concentrations has been carried out under the assumption of an isotopologue distribution from the 2.5 ppm mixture due to the natural isotopic distribution. This assumption has been supported by strength comparisons of the same transitions from different isotopologues. The dotted lines are the upper and lower 95% confidence levels for the fit. Corresponding to a signal-to-noise ratio of 2, the detection limit is at about 0.8 ppt. Due to the application of boxcars, a single dilution series can just cover a certain range of concentrations. In principle, the behavior of data points is linear to about 100 ppb. For higher concentration self-quenching of NO has to be taken into account. Furthermore, the $^{14}N^{18}O$ transition has been used to monitor the output of the isotopologue from exhaled air in an online measurement [30]. Comparable procedures have been performed for $^{15}N^{16}O$ [7, 31, 33]. Hence, application of LIF is an excellent tool for highly sensitive isotopologue selective detection of NO. ^{15}N-labeled drugs or amino acids, e.g. L-arginine which is metabolized to $^{15}N^{16}O$, can be used to reveal reaction pathways and temporal conversion in biological systems [6]. This application has been enriched by providing a tool for the selective observation of $^{14}N^{18}O$ as a metabolite from ^{18}O-labeled agents.

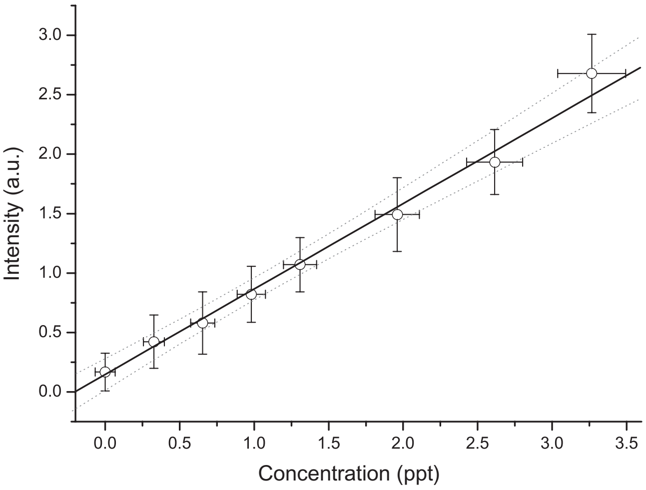

Figure 3. Dilution series for $^{14}N^{18}O$ with Ar. The straight line is a fit taking into account the errors of both coordinates. The dotted lines are the upper and lower 95% confidence levels for the fit.

Further studies evaluated the suitability of the $A^2\Sigma^+(v'=1) \leftarrow X^2\Pi_\Omega(v''=0)$ transition around 215.0 nm for the application on isotopologue selective detection of NO. Again, REMPI measurements provided spectroscopic windows for interference-free detection of the minor isotopologues. We introduce here the red end of the $AX(v'=1)$ transition. In this region between 215.42 and 215.51 nm, $^{14}N^{18}O$ can be observed without interference. Therefore, this spectral region is extremely suitable for an isotopologue selective detection. The previously described LIF setup has been used for these experiments with Coumarin 120 as dye. The measurements have been performed with 2.5 ppm NO in N_2 at cell pressures of 10 mbar. Figure 4 shows a measured spectrum of this region (positive values). The upside down solid black line is a simulation for $^{14}N^{18}O$ $AX(v'=1)$ of the $^OP_{12}(J'')$ branch. This region is interfered by the extremely weak

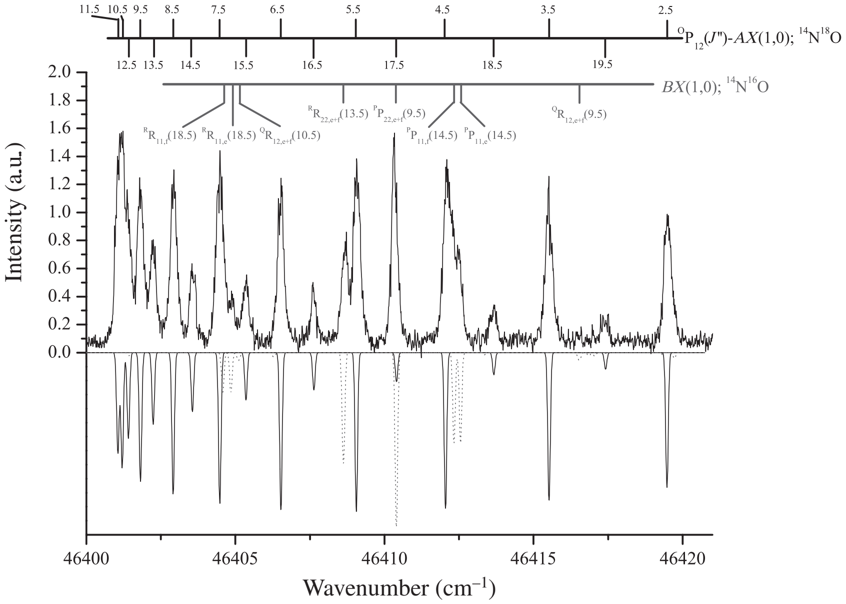

Figure 4. Spectrum between 215.42 and 215.51 nm showing the $^{O}P_{12}(J'')$ branch of $^{14}N^{18}O$ from $A^2\Sigma^+(v'=1) \leftarrow X^2\Pi_\Omega(v''=0)$ (measured spectrum with positive values: calculation in black upside down) and some transitions from $B^2\Pi(v'=1) \leftarrow X^2\Pi_\Omega(v''=0)$ of $^{14}N^{16}O$ (dotted line, upside down).

$B^2\Pi(v'=1) \leftarrow X^2\Pi_\Omega(v''=0)$ transition whose simulation is displayed upside down as dotted lines. Very precise fittings concerning the estimation of spectroscopic constants for the different isotopologues can be performed in this region for the $AX(1,0)$ of $^{14}N^{18}O$ [30] and the $BX(1,0)$ of $^{14}N^{16}O$. The fitting procedure provided for the excited $B^2\Pi(v'=1)$ state of $^{14}N^{16}O$ a rotational constant $B = 1.10310\,\text{cm}^{-1}$ and a spin–orbit coupling constant $A = 33.170\,\text{cm}^{-1}$. Concerning an isotopologue-specific detection of $^{14}N^{18}O$, the $^{O}P_{12}(6.5)$ and $^{O}P_{12}(3.5)$ transitions are most suitable.

4. Conclusions and perspectives

(1+1) REMPI has been applied to reveal spectroscopic windows from $A^2\Sigma^+(v'=0) \leftarrow X^2\Pi_\Omega(v''=0)$ for the isotopologue selective detection of NO. These regions have been studied in more detail by the application of an LIF experiment. As shown, it is possible to detect $^{14}N^{16}O$, $^{15}N^{16}O$ and $^{14}N^{18}O$ separately without interference with each other down to concentrations in the sub-ppt region. The detection limit for $^{14}N^{18}O$ has been improved to 0.8 ppt. This technique can be used for label studies with drugs or amino acids metabolizing NO to reveal reactive pathways in biological systems as well as its temporal evolution. An application is the non-invasive detection of NO in exhaled air.

It has been shown that specific detection of NO is also possible in the 215 nm excitation region in addition to the conventional 226 nm region by application of the $A^2\Sigma^+(v'=1) \leftarrow X^2\Pi_\Omega(v''=0)$ transition for LIF. The higher vibrational state gives rise to a better separation of the isotopologue band heads, which results in a bigger shift of the spectra at the red end of the spectrum compared to $AX(0,0)$. Furthermore, precise LIF measurements can provide exact spectroscopic constants for the calculation of rovibronic states from $^{14}N^{16}O$, $^{15}N^{16}O$ and $^{14}N^{18}O$. The 215 nm region is interfered by the weak $B^2\Pi(v'=1) \leftarrow X^2\Pi_\Omega(v''=0)$ transition of $^{14}N^{16}O$. Calculations from measured transitions provided a rotational constant $B = 1.10310\,\text{cm}^{-1}$ and a spin–orbit coupling constant $A = 33.170\,\text{cm}^{-1}$ for the excited $B^2\Pi(v'=1)$ state of $^{14}N^{16}O$. In the future we will apply the REMPI setup in combination with a molecular beam to observe cold NO with the aim of separated $AX(1,0)$ and $BX(1,0)$ states for characterization of the latter and calculation of the band head.

Acknowledgments

This work was supported by the Braunschweig International Graduate School of Metrology.

References

[1] Furchgott R F 1999 Endothelium-derived relaxing factor: discovery, early studies, and identification as nitric oxide (nobel lecture) *Angew. Chem. Int. Ed. Engl.* **38** 1870–80

[2] Ignarro L J, Buga G M, Wood K S, Byrns R E and Chaudhuri G 1987 Endothelium-derived relaxing factor produced and released from artery and vein is nitric oxide *Proc. Natl Acad. Sci. USA* **84** 9265–9

Ignarro L J 2003 Nitric oxide: a unique endogenous signalling molecule in vascular biology; Nobel lecture 1998 *Nobel Lectures, Physiology and Medicine 1996–2000* ed H Jörnvall (Singapore: World Scientific) pp 178–98

Murad F 2003 Discovery of some of the biological effects of nitric oxide and its role in cell signaling, Noble lecture 1998 *Nobel Lectures, Physiology and Medicine 1996–2000* ed H Jörnvall (Singapore: World Scientific) pp 210–33

[3] Moncada S, Palmer R M and Higgs E A 1991 Nitric oxide: physiology, pathophysiology and pharmacology *Pharmacol. Rev.* **43** 109–42

[4] Kharitonov S A and Barnes P J 2000 Clinical aspects of exhaled nitric oxide *Eur. Respir. J.* **16** 781–92

[5] Högman M and Meriläinen P 2007 Extended NO analysis in asthma *J. Breath Res.* **1** 024001

[6] Lauenstein J and Gericke K-H 2005 Isotope selective detection of nitric oxide in human exhalation *Breath Analysis for Clinical Diagnosis and Therapeutic Monitoring* ed A Amann and D Smith (New Jersey: World Scientific) chapter B, pp 161–9

[7] Lauenstein J 2006 Isotopenselektiver Nachweis von biologisch freigesetztem Stickstoffmonoxid *PhD Thesis* University of Braunschweig

[8] Bruch-Gerharz D, Ruzicka T and Kolb-Bachofen V 1998 Nitric oxide and its implications in skin homeostasis and disease—a review *Arch. Dermatol. Res.* **290** 643–51

[9] Lamattina L, García-Mata C, Graziano M and Pagnussat G 2003 Nitric oxide: the versatility of an extensive signal molecule *Annu. Rev. Plant Biol.* **54** 109–36

[10] Delmas R, Serca D and Jambert C 1997 Global inventory of NO_x sources *Nutr. Cycling Agroecosys.* **48** 51–60

[11] De Laeter J R, Böhlke J K, De Bièvre P, Hidaka H, Peiser H S, Rosman K J R and Taylor P D P 2003 Atomic weights of the elements: Review 2000 *Technical Report 6, IUPAC Technical Report*

[12] Bollinger M J, Birks J W and Gergory J K 2000 Nitric oxide detector *United States Patent* 6635415

[13] Robinson J K, Bollinger M J and Birks J W 1999 Luminol/H_2O_2 chemiluminescence detector for the analysis of nitric oxide in exhaled breath *Anal. Chem.* **71** 5131–6

[14] Bakhirkin Y A, Kosterev A A, Roller C, Curl R F and Tittel F K 2004 Mid-infrared quantum cascade laser based off-axis integrated cavity output spectroscopy for biogenic nitric oxide detection *Appl. Opt.* **43** 2257–66

[15] Halmer D, von Basum G, Horstjann M, Hering P and Mürtz M 2005 Time resolved simultaneous detection of ^{14}NO and ^{15}NO via mid-infrared cavity leak-out spectroscopy *Isot. Environ. Health Stud.* **41** 303–11

[16] Mürtz P, Menzel L, Bloch W, Hess A, Michel O and Urban W 1999 LMR spectroscopy: a new sensitive method for on-line recording of nitric oxide in breath *J. Appl. Physiol.* **86** 1075–80

[17] Koch M, Luo X, Mürtz P, Urban W and Mörike K 1997 Detection of small traces of $^{15}N_2$ and $^{14}NO_2$ by Faraday LMR spectroscopy of the corresponding isotopomers of nitric oxide *Appl. Phys.* B **64** 683–8

[18] Harren F J M, Cotti G, Oomens J and te Lintel Hekkert S 2000 *Photoacoustic Spectroscopy in Trace Gas Monitoring* (New York: Wiley)

[19] Carini M, Aldini G, Stefani R, Orioli M and Facino R M 2001 Nitrosyslhemoglobin, an unequivocal index of nitric oxide release from nitroaspirin: *in vitro* and *in vivo* studies in the rat by ESR spectroscopy *J. Phrm. Biomed. Anal.* **26** 509–18

[20] Sich I and Russow R 1999 ^{15}N analysis of nitric oxide and nitrous oxide by cryotrap enrichment using a gas chromatograph quadrupole mass spectrometer and its application to ^{15}N-tracer investigations of NO/N_2O formation in soil *Rapid Commun. Mass Spectrom.* **13** 1325–8

[21] Tsikas D, Sandmann J, Savva A, Luessen P, Boger R H, Gutzki F M, Mayer B and Frolich J C 2000 Assessment of nitric oxide synthase activity *in vitro* and *in vivo* by gas chromatography-mass spectrometry *J. Chromatogr. B: Biomed. Sci. Appl.* **742** 143–53

[22] Amiot C, Bacis R and Guelachvili G 1978 Infrared study of the $X^2\Pi v = 0, 1, 2$ levels of $^{14}N^{16}O$. Preliminary results on the $v = 0, 1$ levels of $^{14}N^{17}O$, $^{14}N^{18}O$, and $^{15}N^{16}O$ *Can. J. Phys.* **56** 251–65

[23] Wang D X, Haridass C and Reddy P S 1996 The gamma ($A^2\Sigma^+$–$X^2\Pi_r$) system of nitric oxide isotopomers *J. Mol. Spectrosc.* **175** 73–84

[24] Danielak J, Domin R, Kępa U, Rytel M and Zachwieja M 1997 Reinvestigation of the emission γ band system ($A^2\Sigma^+$–$X^2\Pi$) of the NO molecule *J. Mol. Spectrosc.* **181** 394–402

[25] Luque J and Crosley D R 1999 Transition propabilities and electronic transition moments of the $A^2\Sigma^+$–$X^2\Pi$ and $D^2\Sigma^+$–$X^2\Pi$ systems of nitric oxide *J. Chem. Phys.* **111** 7405–15

[26] Freedman R and Nicholls R W 1980 Notes: molecular constants for the $v'' = 0$ ($X^2\Pi$) and $v' = 0, 1$ ($A^2\Sigma^+$) levels of the NO molecule and its isotopes *J. Mol. Spectrosc.* **83** 223–7

[27] Luque J and Crosley D R 1995 Electronic transition moment for the $B^2\Pi$–$X^2\Pi$ system of NO *J. Quant. Spectrosc. Radiat. Transfer* **53** 189–200

[28] Gadd G E and Slanger T G 1990 NO ($B^2\Pi$) radiative lifetimes: $v = 0$–6 *J. Chem. Phys.* **92** 2194–202

[29] Piper L G, Tucker T R and Cummings W P 1991 Electronic transition moment variation and einstein coefficients for the NO($B^2\Pi$–$X^2\Pi$) system *J. Chem. Phys.* **94** 7667–76

[30] Mitscherling C, Maul C and Gericke K-H 2009 Laser-induced fluorescence spectroscopy of $^{14}N^{18}O$ and its application to breath analysis *Isot. Environ. Health Stud.* **45** 59–67

[31] Mitscherling C, Lauenstein J, Maul C, Veselov A A, Vasyutinskii O S and Gericke K-H 2007 Non-invasive and isotope-selective laser-induced fluorescence spectroscopy of nitric oxide in exhaled air *J. Breath Res.* **1** 026003

[32] Western C M *Pgopher, a Program for Simulating Rotational Structure* University of Bristol. http://pgopher.chm.bris.ac.uk/

[33] Lauenstein J 2002 In situ Nachweis von ^{15}NO in der Atemluft *Diplomarbeit* TU-Braunschweig